Evolution of resistance to COVID-19 vaccination with dynamic lockdown

Martin Nowak (martin_nowak@harvard.edu)
Harvard University https://orcid.org/0000-0001-5489-0908

Gabriela Lobinska
Weizmann Institute of Science

Ady Pauzner
Tel Aviv University

Arne Traulsen
Max Planck Institute for Evolutionary Biology https://orcid.org/0000-0002-0669-5267

Yitzhak Pilpel
Weizmann Institute of Science

Article

Keywords: COVID-19, pandemic, vaccinations, immunology

Posted Date: July 13th, 2021

DOI: https://doi.org/10.21203/rs.3.rs-646895/v1

Version of Record: A version of this preprint was published at Nature Human Behaviour on February 24th, 2022. See the published version at https://doi.org/10.1038/s41562-021-01281-8.

Evolution of resistance to COVID-19 vaccination with dynamic lockdown

Gabriela Lobinska*[1], Ady Pauzner[2], Arne Traulsen[3], Yitzhak Pilpel*[1], Martin A Nowak*[4]

1 Department of Molecular Genetics, Weizmann Institute of Science, Rehovot 76100, Israel

2 Berglas School of Economics, Tel Aviv University, Tel Aviv 69978, Israel

3 Department of Evolutionary Theory, Max-Planck-Institute for Evolutionary Biology, August-Thienemann-Str. 2, 24306 Ploen, Germany

4 Department of Mathematics, Department of Organismic and Evolutionary Biology, Harvard University, Cambridge MA 02138, USA

The COVID-19 pandemic has led to an unprecedented global response in terms of social lockdown in order to slow the spread of the virus [1,2]. Currently the greatest hope is based on world-wide vaccination[3,4]. The expectation is that social and economic activities can gradually resume as more and more people become vaccinated. Yet, a relaxation of social distancing that allows increased transmissibility, coupled with selection pressure due to vaccination, will likely lead to the emergence of vaccine resistance [5]. Here we analyze the evolutionary dynamics of COVID-19 in the presence of dynamic lockdown and in response to vaccination. We use infection and vaccination data of 6 different countries (Israel, US, UK, Brazil, France and Germany) to assess the probability and timing for the wave of vaccine resistant mutant[2]. For slow vaccination rates, resistant mutants will appear inevitably even if strict lockdown is maintained. For fast vaccination rates (such as those used in Israel) the emergence of the mutant can be prevented if strict lockdown is maintained during vaccination. Our mathematical results provide quantitative guidelines for a combined vaccination and lockdown policy that minimizes the probability of emergence of vaccine resistance variants for current and future vaccination programs.

The COVID-19 pandemic has had a devastating effect on global health and economy. Since the identification of the first SARS-COV-2 case in December 2019, 178.71 million infections have been recorded and at least 3.86 million people have died as a result of the infection (as of June 2021)[2]. The increased mortality and complication rates of SARS-COV-2[1] compared to the mild diseases caused by seasonal coronaviruses, such as HCoV-229E[6], have led to unparalleled governmental and individual-level responses in order to reduce the number of SARS-COV-2 infections.

Since the beginning of the pandemic, it has become clear that non-pharmaceutical interventions (NPI), such as lockdowns, are economically and socially unsustainable in the long run. Periodical loosening and tightening of social distancing measures, which present an attempt at balancing economical and sanitary considerations, have led to waves of increase and decrease in the number of SARS-COV-2 infections per day[2] (see **Figure 1A**). Therefore, much hope has been placed on vaccine development, which would allow the immunization of a large fraction of the population, thereby substantially reducing mortality and potentially achieving herd immunity, which could in principle eradicate SARS-COV-2 altogether.

Mass vaccination campaigns have been launched in many countries (see **Figure 1B**), most notably Israel and the UK (both more than 60% of vaccinated population) and the US and Germany (both more than 50% of vaccinated population). Currently, four companies are producing vaccines that have been approved for emergency use either by the Food and Drug Administration (FDA)[3] or by the European Medicines Agency (EMA)[4]: Pfizer-Biontech, Moderna, AstraZeneca and Johnson & Johnson/Janssen Pharmaceuticals. Several other vaccines are also used outside of the European Union and the USA: Gamaleya (Sputnik V), Sinopharm Beijing, Sinovac, Sinopharm-Wuhan and Bharat-Biotech (Covaxin)[7].

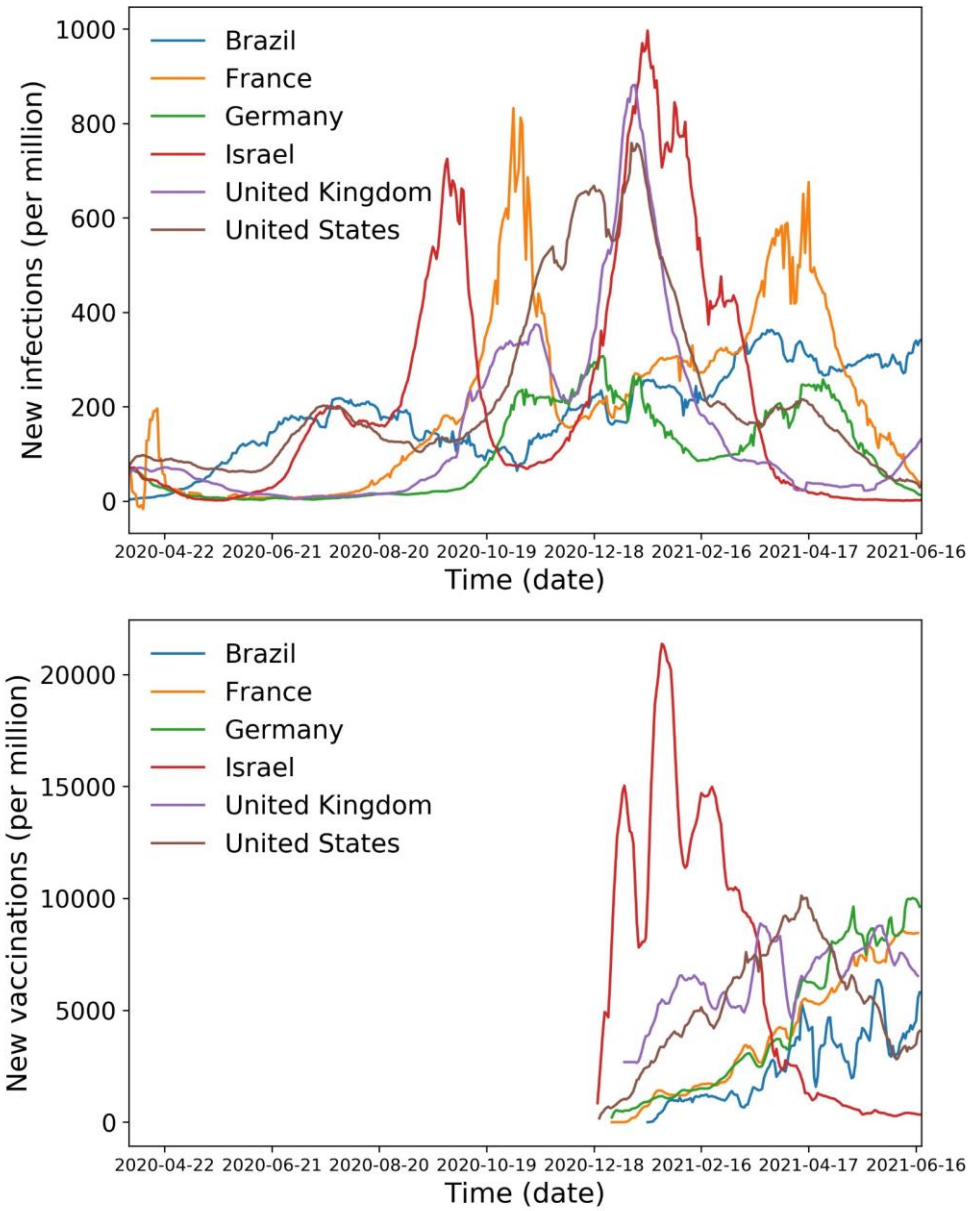

Figure 1: New SARS-CoV2 cases per day per million and number of vaccinations against SARS-CoV2 per day per million in France, Germany, USA, Israel, Brazil and UK. (A) In an attempt to balance economic and sanitary considerations, these six countries have gone through several cycles of loosening and tightening government-imposed restrictions, resulting in periodical increases and decreases in the number of SARS-CoV2 infections per day. The so-called "British variant", identified in November 2020, is most probably responsible for the increase in the number of infections in the UK and Israel at that time. **(B)** Large scale vaccination programs commenced in December 2020. At the peak, Israel vaccinated more than 20,000 people per million (2%) per day. The vaccination rate then decreased in April 2021 as most eligible individuals had been vaccinated.

However, the identification of new SARS-COV-2 variants has cast a shadow over the expectation of a swift end of the pandemic[8,9]. The so-called "British" variant (B.1.1.7), now termed α, and "South African" variant (501.V2), now termed β, have been shown to be neutralized to a lesser extent by convalescent and vaccinee sera[10], although experiments on non-human primates have shown that this decrease might not necessarily cause a decrease in immunity[11]. Structural studies have mapped and predicted mutations that lead to antibody escape[12–14]. As vaccination around the world progresses, the continued evolution of SARS-COV-2 could eventually give rise to a fully vaccine resistant variant. Such a variant could quickly spread due to its ability to infect vaccinated and recovered in addition to fully susceptible individuals. The question of emergence of vaccine resistance has already been the subject of many research papers[15–18].

What policy could be exercised that would minimize the chance of emergence of vaccine resistant strains? Policymakers can vary the extent of social distancing imposed and regimes of vaccine administration. The critical biological parameters on the other hand include the infectivity of the various strains and the rate of mutation of the virus that may ultimately lead to emergence of a resistant strain. Here we introduce a mathematical model that examines various combinations of these parameters. Our model helps to design optimal policies that would minimize the chance of emergence of resistant strains or maximize the time until their occurrence.

Our paper is an addition to the extensive body of work that has been performed in the past year in order to understand the spread and evolution of SARS-COV-2[19–25]. SARS-COV-2 research has drawn on a very long history of epidemiological research[26,27,36–38,28–35]. Due to the global and urgent nature of the pandemic, many studies that could inform policy-making have been conducted[5,39,48,40–47].

In order to understand the evolutionary potential of the virus in response to a vaccination program we study a stochastic model for infection dynamics and virus evolution in the presence of varying degrees of social lockdown and different vaccination rates. We

distinguish between a wild-type virus (WT) and a vaccine resistant mutant virus (MT). The vaccine is effective against the WT strain, while the MT strain evades immunity induced by the vaccine either partially or completely. We build upon the mathematical framework of the Susceptible-Infected-Removed (SIR) model from epidemiology [32,49], albeit with considerable adjustments necessitated by the specific problem at hand . Our model keeps track of people who are susceptible, infected by WT or MT, recovered from WT or MT, vaccinated or unvaccinated (**Figure 2**).

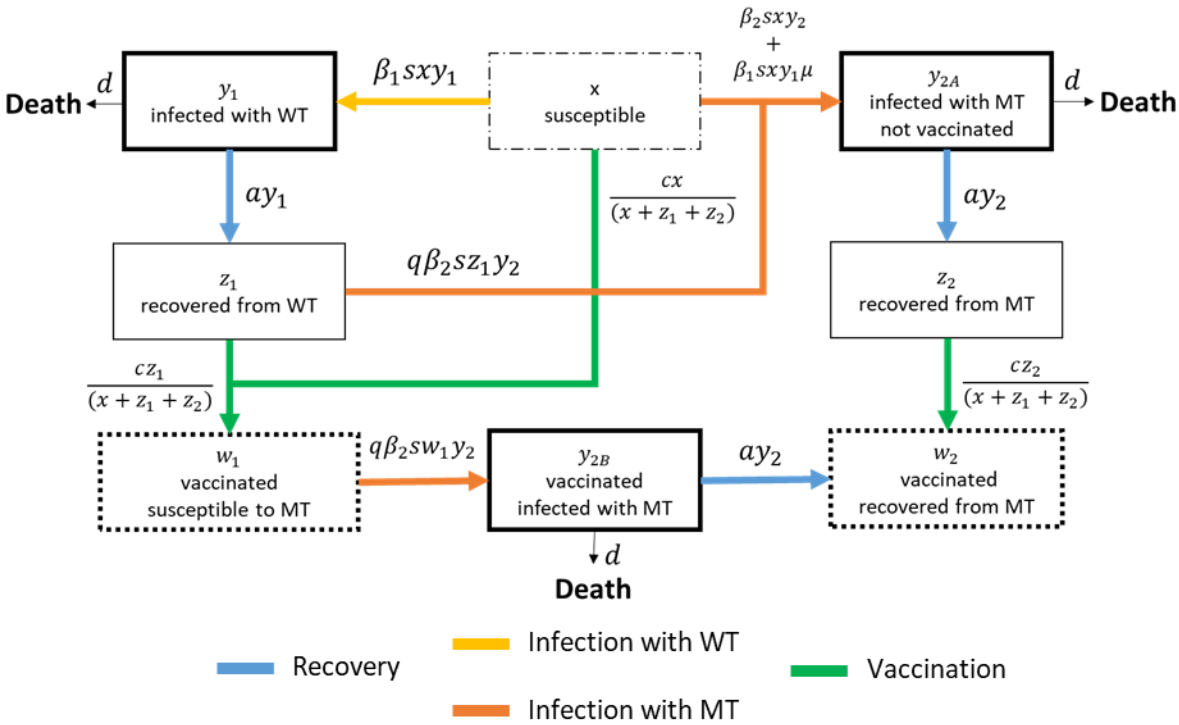

Figure 2: Infection dynamics, vaccination and resistance. Susceptible individuals (x) can be infected by wildtype (WT) or mutant (MT) virus. Infected people (y_1, y_{2A}, y_{2B}) can die (with rate d) or recover (with rate a). People recovered from WT or vaccinated against WT can be infected by MT. People recovered from MT cannot be infected by WT. We assume equal infectivity, recovery and death rates for both WT and MT. Vaccination occurs at rate c per day for all unvaccinated individuals (excluding those that are currently in active infection). Mutation happens (at rate μ) when exposure to a WT infected individual (y_1) results in the generation of a MT infected individual. Since μ is small, we neglect the term $1-\mu$. The rates of these events are indicated on the arrows and are used in the Gillespie algorithm implementing the stochastic dynamics.

112 Crucially, we assume there is a dynamic lockdown guided by the number of new infections
113 per day. As that number exceeds a threshold, governmental rules and individual
114 responses reduce social activity. If the number of new infections falls below this
115 threshold, the lockdown is somewhat relaxed and some people stop following the rules,
116 thereby allowing higher transmission of the virus. We simulate these dynamics as a
117 stochastic process. In consequence, we obtain fluctuating numbers of new infections per
118 day. We introduce mass vaccination at alternative fixed rates. Then we compute the
119 probability and timing of the wave of infection caused by the spontaneous emergence of
120 a vaccine resistant virus.

121 In our approach, the mutation rate μ denotes the probability that a WT-infected individual
122 will infect a susceptible individual with the MT strain. The exact value of this probability
123 is currently unknown and complex to obtain empirically. For the simulations and
124 calculations reported in this paper we therefore consider a wide range of mutation rates.
125 From our model, we also derive an upper bound for the mutation rate using the fact that
126 no wave of a vaccine-resistant variant has occurred up until now. Note that this rate can
127 be very different from the per-base mutation rate of SARS-COV-2, which is about 10^{-5}.

128

129 DYNAMICS OF VIRAL INFECTION AND EVOLUTION

130 Our model keeps track of eight different variable states: individuals who are susceptible
131 (x), infected with WT (y_1), non-vaccinated and infected with MT (y_{2A}), vaccinated and
132 infected with MT (y_{2B}), recovered from WT (z_1), recovered from MT (z_2), vaccinated but
133 susceptible to MT (w_1), vaccinated and recovered from MT (w_2); see **Figure 2**.

134 The WT strain can infect susceptible individuals (x), converting them to individuals
135 infected with WT (y_1) at rate β_1. A mutation can occur with probability μ. In this case, a
136 WT infected individual infects a susceptible individual (x) with a mutated version of the
137 virus, in a mutation that have taken place in the infecting individual, thus converting the
138 susceptible to a MT infected individual (y_{2A}). WT infected individuals either recover with

rate a and become immune to future WT infection (z_1) or die at rate d. Susceptible individuals (x) and individuals recovered from WT (z_1) can become vaccinated individuals (w_1). The parameter c denotes the number of individuals vaccinated per day. Hence, the rates of vaccination of x, z_1 and z_2 are respectively $cx/(x + z_1 + z_2)$, $cz_1/(x + z_1 + z_2)$ and $cz_2/(x + z_1 + z_2)$. For simplicity we assume single-dose vaccination; for a double dose vaccine our model would describe the application of the second dose ignoring partial immunity caused by the first dose; extension of our model to a full two dose vaccination protocol is straightforward.

At rate β_2, the MT strain infects susceptible individuals (x), WT recovered individuals (z_1) and vaccinated individuals who are not immune to MT (w_1). MT infected individuals either recover with rate a and become immune to future MT and WT infection (z_2) or die at same death rate d as with the WT strain, i.e. assuming no difference in lethality between the two strains. We assume one-way cross-immunity induced by the viral strains: the MT strain can infect individuals that have recovered from WT or that have been vaccinated against WT, but the WT strain cannot infect individuals that have recovered from the MT. In practice, the WT strain becomes extinct soon after the appearance of the MT strain, meaning that the number of individuals recovered from MT that could become infected with WT is negligible. We note that our MT strain escapes both from the immunity that is induced by natural infection with WT and the immunity induced by vaccination against WT.

We need to distinguish between MT infected individuals that are or are not vaccinated: y_{2B} and y_{2A}, respectively. Upon recovery the former will not be vaccinated (again), while the latter will be vaccinated.

We also study partial immunity to the MT strain which can be acquired by recovery from WT infection or by vaccination. For partial immunity, the corresponding infection rates are multiplied by a parameter q, which is between 0 and 1. If $q = 1$ then WT infection or vaccination confers no immunity to MT at all; the mutant escapes completely. For $0 < q < 1$, the MT is a partial escape mutant. For $q = 0$, the MT does not escape at all.

Lockdown measures are implemented by multiplying the infectivity coefficients of each strain by a social activity parameter s which ranges in $[0,1]$. Unconstrained social interaction means $s = 1$, while $s = 0$ would be complete lockdown. The population tolerates a certain number of new infections, L, per day. Each day, if the number of new infections exceeds L, then s is decreased by a random, uniformly distributed number between 0 and 0.1. If the number of new infections is less than L, then s is increased by a random, uniformly distributed number between 0 and 0.1. In any case, s cannot decrease below 0.05 or increase above 1.

As an example, the rate of infection of the recovered from WT z_1 by the MT strain infected individuals y_2 is multiplied both by the lockdown coefficient s and the partial immunity coefficient q – hence this rate is given by $q\beta_2 s w_1 y_2$.

COMPUTATIONAL IMPLEMENTATION AND DATA

A Gillespie algorithm is commonly used to simulate stochastic systems with high variation in waiting times between consecutive events[50–53]. In our model the population is represented as a vector of length eight, corresponding to the eight categories. The rates of all possible events (infection, recovery, death, mutation and vaccination) are calculated. The time of the next event in the model is drawn from an exponential distribution, with parameter dependent on the sum of all event rates and an event is chosen, with probability proportional to its rate. The population is updated according to the event that occurred. The simulation is stopped when there are no more infected individuals in the population. The algorithm is presented in pseudocode in the **Appendix**, along with a table of the possible events of the model and their default rates.

In order to achieve feasible computation time and resources, we simulated populations of size up to $N = 10^6$. The results of those simulations can be scaled to larger population sizes by considering a population of for example $N = 10^7$ as $m = 10$ "batches" of 10^6 individuals, and computing the results for $N = 10^7$ as $1 - (1 - p)^m$, where p is the proportion of runs where the MT strain took over. **Figure S1** shows the strong agreement

between simulated results and the results scaled from simulations with smaller population sizes.

For all our simulations, we have endeavored to use real world data for all model parameters. In particular, infection and vaccination data has been obtained from the database *Our World in Data* [2] (OWID) and downloaded on June 19th, 2021.

In our simulation, since the number of new infections each day is constant, the number of susceptible individuals decreases linearly with slope $-L/a$. Vaccination of both susceptible and recovered individuals proceeds at rate c. The social activity parameter, s, increases as more and more individuals become immunized either by infection or by vaccination. The WT reproductive rate, R_{WT} , is maintained at 1 as long as the MT has not appeared. The MT reproductive rate, R_{MT} , increases with the social activity parameter s until the MT strain takes over. After MT takeover, the MT reproductive rate R_{MT} is buffered at 1 by the dynamic lockdown (see **Figure 3** and **Methods**).

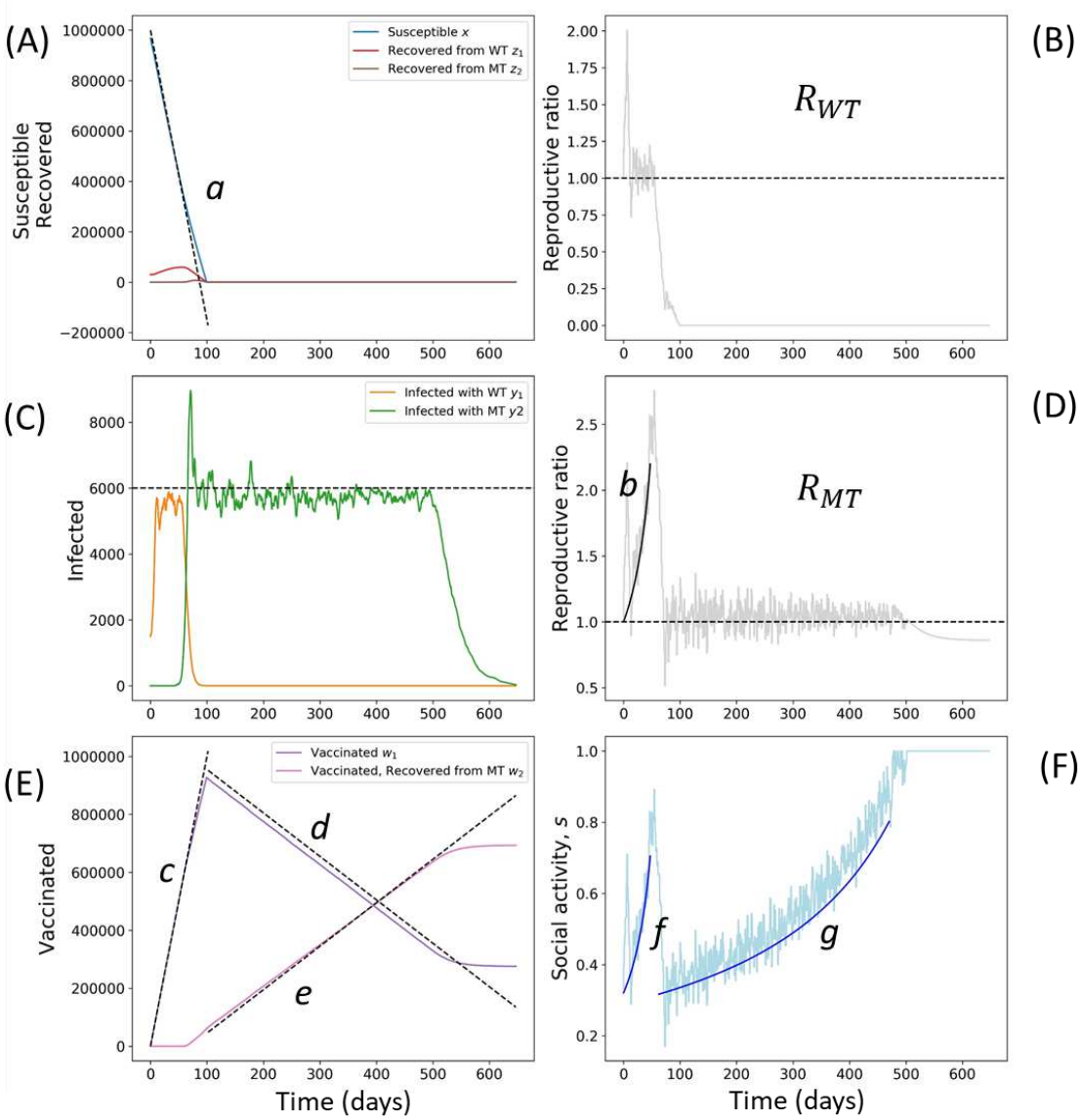

Figure 3: Evolution of resistance in presence of vaccination. (A) Before MT takeover, the decline in susceptible individuals (x) can be approximated by a linear function with slope equal to the vaccination rate c. Since vaccination is fast, individuals recovered from WT and non-vaccinated individuals recovered from MT are few. The equation of line (a) is $x(t) = x(0) - ct$ for $t < t^*$ where t^* is the time of takeover of the MT. (B) The reproductive rate R_{WT} is maintained at around 1 by dynamic lockdown. After mutant takeover, R_{WT} is less than 1, since the lockdown is now adjusted to the population susceptible to the MT strain. (C) The number of active WT infections before takeover and of active MT infections after takeover, is fluctuating around L/a until herd immunity to the MT is reached. (D) Before MT takeover, the reproductive rate of the MT grows as (b) $R_{MT} = \beta_2(x(t) + z_1(t) + w_1(t))/a$. After takeover, R_{MT} is maintained around 1. (E) The number of vaccinated individuals (w_1) first increases linearly with slope equal to the vaccination rate. After MT takeover, the number of individuals vaccinated to the WT and recovered from MT (w_2)

increased linearly with slope L. The equations of the lines are given by (c) $w_1(t) = ct$ for $t < t^*$ (d) $w_1(t) = w_1(t^*) - L(t - t^*)$ for $t > t^*$ (e) $w_2(t) = L(t - t^*)$ for $> t^*$. (F) Before MT takeover, the dynamic lockdown is adjusted to the WT. As the number of individuals immune to WT grows, social activity increases. When the MT emerges, lockdown measures are reinstated. Subsequently, social activity increases as the population immune to the MT grows. The equations for the lines given by (f) $s(t) = a/\beta_1 x(t)$ for $t < t^*$; (g) $s(t) = a/\beta_2(x(t) + z_1(t) + w_1(t))$ for $> t^*$.

We performed 1000 runs of the stochastic simulation for each combination of parameters reflecting realistic values of the two model parameters determined by governmental policy: the tolerated number of infections per day, L, and the vaccination rate per day, c. Each square of the color map shown in **Figure 4** reflects the average value of these 1000 runs, which were performed for a population of $N = 10^6$ and then scaled to $N = 10^7$ and $N = 10^8$. At each combination of L and c the color maps denote the predicted probability of a mutant take over. We perform computations using $q = 1$ and $q = 0.4$ for complete and partial immune evasion by the mutant.

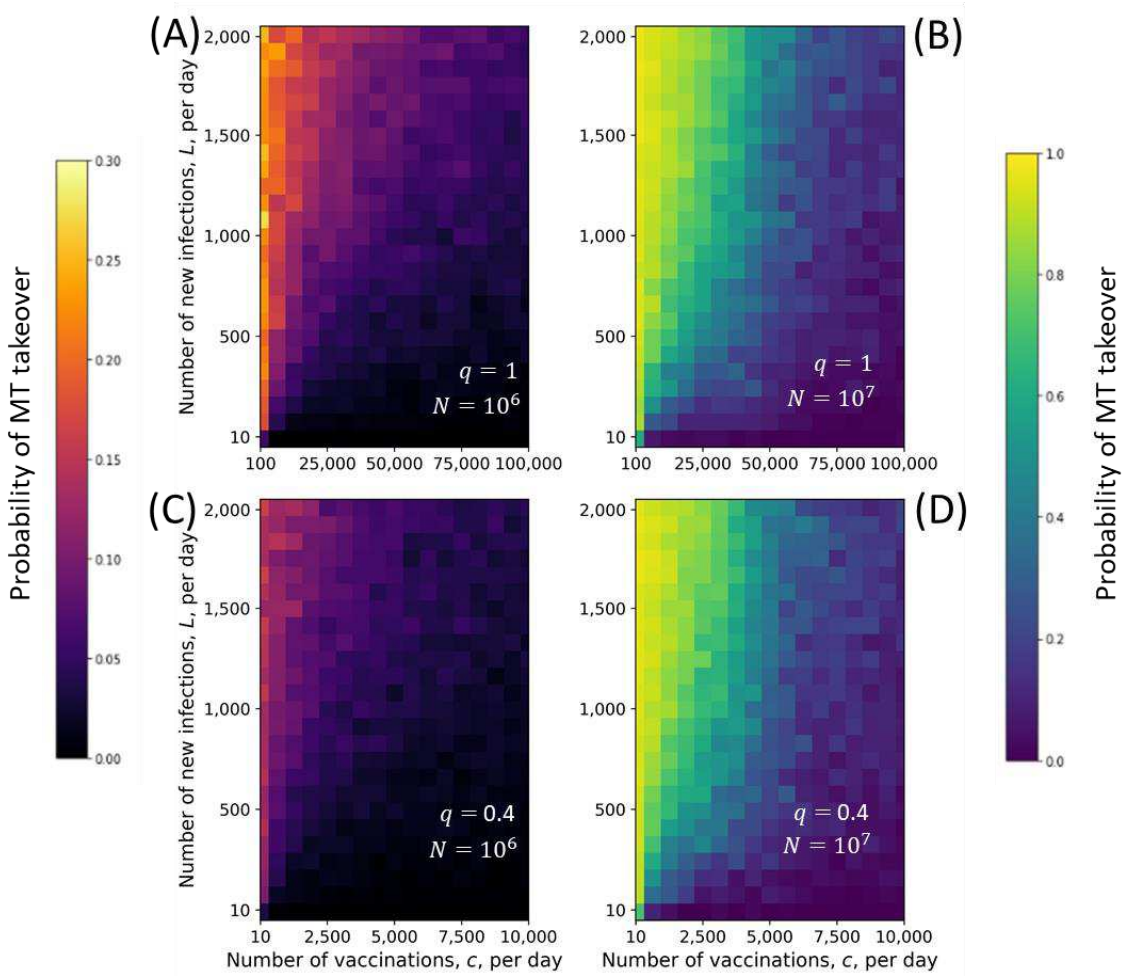

Figure 4: Probability of emergence of resistance. For each square of the color maps, the proportion of runs (out of 1000 runs) where the number of individuals infected with the MT strain exceeded the number of individuals infected with the WT strain is recorded. All simulations are run for a population size of $N = 10^6$, then scaled to obtain the results shown for $N = 10^7$. Results for color maps (B) and (D) were scaled according to $(1 - (1 - p)^{10})$, where *p* is the proportion of runs where the MT strain took over. We observe a triangular shape of (L, c) parameter sets for which the MT strain takes over, indicating that high vaccination rates can be safely associated with more lenient social distancing measures. On the other hand, very slow vaccination cannot be compensated by any strength of lockdown. Partial immunity to the WT strain (panels (A) and (C)) does not affect the shape of the parameter space where we observe MT takeover, but reduces its probability.

Allowing a large amount of infection cases and slow vaccination results is almost certain takeover of the MT strain. On the other hand, very fast vaccination coupled with a low number of tolerated new infections per day can prevent emergence of the MT. Partial immune evasion ($q = 0.4$) of the mutant slightly reduces the probability of its takeover. Note that the shape of the parameter space where we observe takeover is similar for $q = 1$ and $q = 0.4$.

REPRODUCTIVE RATIO OF THE MUTANT AND PROBABILITY OF TAKEOVER

In **Figure 5** we show detailed data from 6 countries together with the estimated reproductive ratio, R_{MT}, of a vaccine resistant mutant and the probability of generating a wave of resistant virus. Data for the number of susceptible individuals $x(t)$, vaccinated individuals $w(t)$, recovered individuals $z(t)$, newly infected individuals $L(t)$, and an estimate for the reproductive rate R_{WT} of the WT can be obtained from *OWID* [2]. The reproductive rate R_{MT} of the escape mutant can be calculated according to:

$$R_{MT}(t) = R_{WT}(t)[x(t) + qw(t) + qz(t)]/x(t) \tag{1}$$

The probability of not producing an escape mutant in a given day is $(1-\mu)^{L(t)}$. The probability of not producing a surviving escape mutant is $(1-\rho(t)\mu)^{L(t)}$, where $\rho(t)$ is the survival probability of a mutant generated on that day. If $R_{MT}(t) < 1$ then $\rho(t) = 0$. If $R_{MT}(t) > 1$ we assume $\rho(t) = 1 - 1/R_{MT}(t)$. The probability that no surviving mutant is generated between time 0 and time t is given by

$$P(t) = \prod_{\tau=0}^{t} [1 - \mu\rho(\tau)]^{L(\tau)} \tag{2}$$

In **Figure 5** we show the reproductive rate of the mutant $R_{MT}(t)$ and the probability $P(t)$ of generating a surviving escape mutant as a function of time. Prior to vaccination the reproductive rate of a potential escape mutant tracks closely that of the WT. As people become vaccinated in large numbers, R_{MT} starts to increase significantly above R_{WT}. Nevertheless, it is possible to keep R_{MT} below one by maintaining some measures of lockdown. (This is the case for Israel and UK). Overall, the probability that Israel generated a vaccine escape mutant (before June 2021) is of order of 1-2 percent (assuming $\mu =$

10^{-7}). For the same mutation rate the corresponding probability for the United States is 32 percent; the United States have a much larger total population size but also many more infections per million people. The corresponding probabilities for Brazil, France, Germany, and UK are 17, 8, 4 and 6 percent (see **Table 1**).

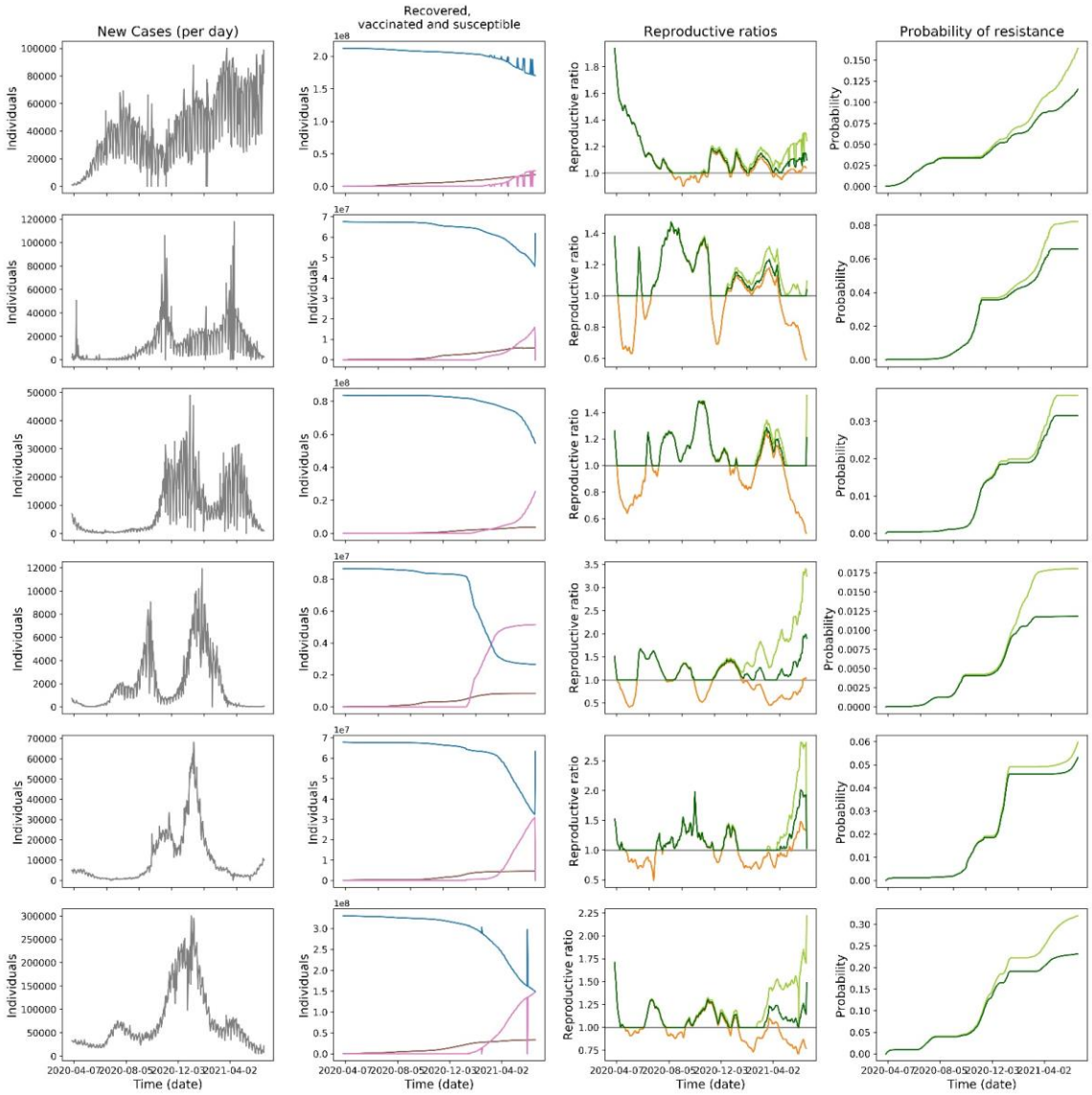

Figure 5: Infection, vaccination data and estimates for reproductive ratios and probability of resistance for Brazil, France, Germany, Israel, the United Kingdom, and the United States. The total number of new cases per day (leftmost column), number of susceptible,, recovered, and vaccinated individuals (second column from left) was downloaded from the *OWID* (Our World In Data) database. We used the *OWID* estimate for the WT reproductive coefficient R_{WT} to calculate the potential MT reproductive coefficient R_{MT} for a full escape mutant ($q = 1$) and a partial escape mutant ($q = 0.4$), (third column). We use Eq. 2 to estimate the probability that an escape mutant would have emerged until a certain date assuming $\mu = 10^{-7}$ (fourth column).

Country	Population size ($\times 10^6$)	Average rate of infection per day per person before vaccination ($\times 10^{-6}$)	Average rate of infection per day per person after vaccination ($\times 10^{-6}$)	Average rate of vaccination per day per person ($\times 10^{-6}$)	Probability of resistance ($\mu = 10^{-7}$)
Brazil	212.6	132	294	2946	0.166
France	68.1	120	319	4440	0.082
Germany	83.8	67	135	4878	0.037
Israel	8.7	120	412	9181	0.018
United Kingdom	67.9	109	187	6358	0.060
United States	331.0	173	246	5533	0.320

Table 1: Calculated probability of emergence of vaccine resistance using real-world data from six countries: Brazil, France, Germany, Israel, the United Kingdom and the United States. The probability of vaccine resistance was calculated using the product formula in Eq. 2 and the data presented in **Figure 5** assuming $\mu = 10^{-7}$.

ESTIMATING THE MUTATION RATE μ

We suggest a method to estimate an upper bound of the mutation rate μ from WT to MT based on the observation that despite a large number of infections since the beginning of the pandemic and including recent vaccination campaigns, no immune evasive mutant has yet taken over. Our method for calculating an upper bound of the mutation rate is potentially applicable for estimating any mutation rate between two phenotypes in an evolving population. The upper bound is computed at any given time point, and can be updated and become tighter if in future evasive strain still does not appear.

For each country, we use Eq. (2) to compute the probability of takeover using data from the beginning of the pandemic up until June 19th 2021 for a wide range of mutation rates. We assume $q = 1$, which means the MT strain is fully immune evasive.

The resulting function for probability of mutant take over (for a given time point) versus mutation rate has a sigmoidal shape, with its midpoint corresponding to the mutation rate for which it is equally probable that the MT strain would have taken over or not. Plugging in data on number of infections in several countries gives an upper bound on the probability of mutant take over and a corresponding estimation of mutation rate per transmission that will result in the emergence of such a mutant. This estimated upper bound on the mutation rate decreases over time as long as more infections do not give rise to a MT strain (see **Figure 6**).

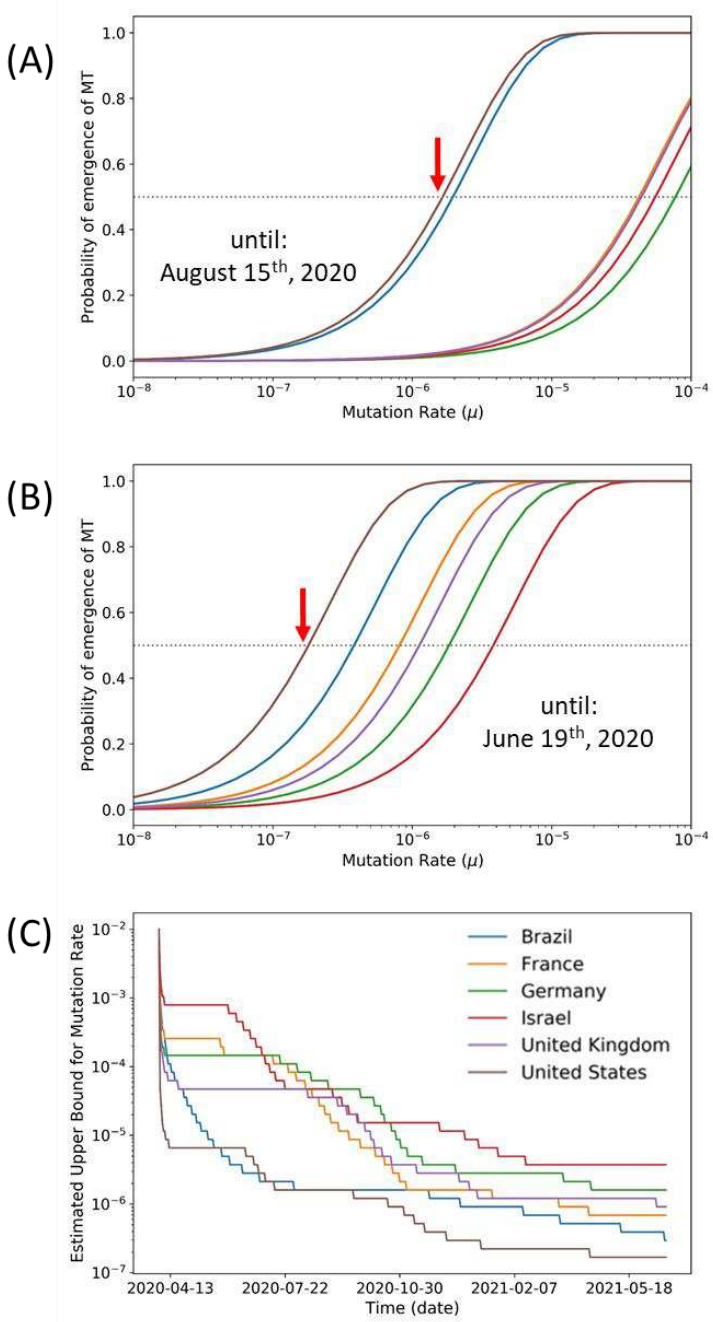

Figure 6: Estimation of mutation rate given that no vaccine resistant mutant has yet taken over. (A,B) Using Eq. 2, we calculate the probability of MT strain takeover for a range of mutation rate values. The probability of MT strain takeover follows a sigmoidal function, where the midpoint is reached for the value of μ where MT strain takeover becomes more probable than not. (C) The midpoint of the function (indicated by a red arrow) describing the probability of MT strain takeover will decrease in value as more and more time passes without the takeover of an MT strain. We can use this value as an upper bound of the mutation rate for our model.

Since the probability of MT takeover (Eq. (2)) is strongly dependent on the number of infections, significant decreases in the estimated values correspond to periods with high infection rates in which, nonetheless, a mutant did not appear. The estimate for the upper bound of the mutation rate is expected to plateau as vaccination campaigns lead to a decrease in the number of infection cases. The estimate of 10^{-6} will decrease further if and when large countries such as the US will advance in the vaccination campaign with no mutant takeover. Using the world infection and vaccination data, we obtain $\mu = 10^{-7}$ as the order of magnitude for the upper bound for the rate at which immune evasive mutants appear. But estimates based on individual countries may be more informative since the world data reflects the average over an extremely heterogeneous population subject to very different policies.

A SIMPLE FORMULA FOR THE ESCAPE PROBABILITY

The dynamic lockdown captured by the social activity parameter $s(t)$ maintains the number of new infections per day fluctuating around a fixed value and thereby buffers the reproductive ratio of the wildtype R_{WT} around 1. The number of active infections is roughly constant and given by L/a, where a is the recovery rate (see **Figure 3**). If vaccination is slow, $c \ll L$, then the change in the number of susceptible, $x(t)$, and recovered individuals, $z_1(t)$, over time can be described by linear functions with slopes proportional to L (see **Methods and Figure S2A**).

Alternatively, for fast vaccination, $c \gg L$, the change in the number of susceptible $x(t)$ and vaccinated individuals $w_1(t)$ can be described by linear functions with slopes proportional to c before MT takeover, and with slopes proportional to L after MT takeover (see **Methods and Figure 3E**). Neglecting vaccination of recovered individuals (which is a reasonable approximation for $c \gg L$) we can write $(t) = N - Lt - ct$, $z(t) = Lt$ and $w(t) = ct$. The time when herd immunity against the WT is reached is given by

$$T_H = \frac{N}{c+L}(1 - \frac{1}{R_0}) \tag{3}$$

During vaccination the reproductive rate of the mutant increases as (see **Methods**)

$$R_{MT}(t) = \frac{N}{N - (L+c)t} \tag{4}$$

The reproductive rate of the MT is initially 1 and increases to R_0 as people recover from WT infection or are vaccinated (see **Figure 3D**). Once a mutant has been generated, the probability of its survival depends on the value of the reproductive rate, $R_{MT}(t)$. The probability that no surviving mutant has appeared before time t, where $t \leq T_H$, can be calculated to be (see **Methods**):

$$P(t) = \exp[-\left(\frac{\mu N}{2}\right)\left(\frac{L}{N}\right)\left(\frac{c+L}{N}\right)t^2] \tag{5}$$

The probability that no surviving mutant has appeared until herd immunity is

$$P(T_H) = \exp\left[-\left(\frac{\mu N}{2}\right)\left(\frac{L}{c+L}\right)\left(1 - \frac{1}{R_0}\right)^2\right] \tag{6}$$

Here $R_0 = \beta N/a$ is the basic reproductive ratio of the WT. The corresponding formulas for partial immune escape mutants are given in the **Methods**. Eq. (6) is in good agreement with the results of exact stochastic simulations (**Figure S3**).

In **Table 2**, we show how the probability and timing of resistance depends on the vaccination rate and the number of new infections per day. We first consider a large country of $N = 10^8$ inhabitants and a mutation rate of $\mu = 10^{-7}$. If 10,000 new infections occur per day and 1 million people are vaccinated per day, then herd immunity is reached in 66 days and the probability of generating a vaccine resistant mutant is about 2 percent. For the same vaccination rate, if 50,000 new infections are tolerated each day, then the probability of generating an escape mutant increases to 10 percent. If 10,000 new infections occur per day but only 100,000 people are vaccinated every day, then the probability of generating vaccine resistance increases to 18 percent.

(A)

Rate of infection l per day per person ($\times 10^{-6}$)	Rate of vaccination c per day per person ($\times 10^{-6}$)	Time to herd immunity, T_H (in days)	Probability of resistance			
			t = 50 days	t = 100 days	t = 200 days	t = T_H
100	1000	606	0.001	0.005	0.022	0.183
100	5000	131	0.006	0.025	-	0.043
200	5000	128	0.013	0.051	-	0.082
500	5000	121	0.034	0.128	-	0.183
100	10,000	66	0.013	-	-	0.022
200	10,000	65	0.025	-	-	0.043
500	10,000	63	0.064	-	-	0.100

$N = 10^8 \quad \mu = 10^{-7}$

(B)

Rate of infection l per day per person ($\times 10^{-6}$)	Rate of vaccination c per day per person ($\times 10^{-6}$)	Time to herd immunity, T_H (in days)	Probability of resistance			
			t = 50 days	t = 100 days	t = 200 days	t = T_H
100	1000	606	0.013	0.053	0.197	0.867
100	5000	131	0.062	0.225	-	0.353
200	5000	128	0.122	0.405	-	0.575
500	5000	121	0.291	0.747	-	0.867
100	10,000	66	0.119	-	-	0.197
200	10,000	65	0.225	-	-	0.353
500	10,000	63	0.481	-	-	0.653

$N = 10^9 \quad \mu = 10^{-7}$

Table 2: Calculated probability of vaccine resistance for a range of vaccination rates and infection rates. We observe of counterintuitive effect of higher probability of resistance along time for higher vaccination rates, but lower probability of resistance overall. See also **Figure S4**.

As the proportion of vaccinated individuals grows, social distancing measures relax, and the probability of emergence of resistance increases. Hence, higher vaccination rates are associated with higher probabilities of resistance after 50, 100 and 200 days (see **Table 2**). However, faster vaccination leads to earlier herd immunity. When herd immunity is reached, there are no more new infections and the cumulative probability of resistance plateaus. Therefore, we observe an interesting counterintuitive effect: the probability of resistance until a fixed time t increases with the vaccination rate c, but the probability of resistance until time T_H when herd immunity is achieved decreases with the vaccination rate c. (see **Table 2 and Figure S4**).

We can derive estimates for the emergence of vaccine resistant strains using current vaccination and infection rates from around the world. If the whole world ($N = 8 \cdot 10^9$) vaccinated as fast as the US ($c = 5000$ per day per million) and had slightly lower infection rates than Germany ($L = 100$ per day per million) then herd immunity would be achieved in $T_H = 131$ days; the probability that a resistant virus was generated and survived by that time would be 0.97 (for $\mu = 10^{-7}$) and 0.29 (for $\mu = 10^{-8}$). If the whole world vaccinated as fast as Brazil ($c = 3000$ per day per million) and had infection rates like the US ($L = 250$ per day per million) then herd immunity would be achieved in $T_H = 205$ days; the probability that a resistant virus was generated and survived by that time would be 0.999 (for $\mu = 10^{-7}$) and 0.75 (for $\mu = 10^{-8}$). Our results underline the importance of maintaining lockdown measures while herd immunity is not achieved and timely distribution of vaccines around the world.

SUMMARY

We have studied evolution of resistance to COVID-19 vaccination in the presence of dynamic lockdown. We use real world data to simulate the spread of the SARS-COV-2 virus. We have performed stochastic simulations and obtained analytical results. In particular, we have derived a simple intuitive formula for the probability of emergence of a vaccine resistant strain over time (Eqs. (5) and (6)).

Our model most closely corresponds to the assumption that immune evasion could be due to a single point mutation. Nevertheless, our estimates of the mutation rate between the wild-type and immune evasive strains could signify that a combination of mutations is needed to achieve immune evasion. Therefore, we have explored lower effective mutation rates than the current estimation for the per-base mutation rate of the SARS-COV-2 virus.

The probability of takeover of an immune evasive strain is mostly dependent on the number of total infection cases that occur during the pandemic. Social distancing measures, such as lockdowns, can delay or event prevent the emergence of the MT strain. Each natural infection is an opportunity for the MT strain to appear and possibly take over. Hence, the main policy goal should be to maximize the proportion of the population which will be immunized to the virus through vaccination as opposed to natural infection.

In terms of policy implications, our result supports the maintenance of social distancing measures until the daily number of infections decreases substantially. Allowing a large number of infections can only be counterbalanced by very high vaccination rates, which ensure that herd immunity is reached before the MT strain can appear and takeover. Furthermore, our result underlines the importance of a worldwide effort to quickly vaccinate as many individuals as possible, especially in highly populated countries with low access to vaccines. Slow, or no vaccination, results in a large number of total cases in these areas and hence the emergence of an MT strain which could then spread over the whole world.

ACKNOWLEDGEMENTS

YP acknowledges the Minerva Foundation and Kimmel Foundation for grant support.

AUTHOR CONTRIBUTIONS

All authors conceived the project and designed the study. GL have written all the code and ran analysis. All authors have written the paper. MN has supervised the project.

CODE AND DATA AVAILABILITY

Available upon request.

430 REFERENCES

431 1. Wu, J. T. *et al.* Estimating clinical severity of COVID-19 from the transmission
432 dynamics in Wuhan, China. *Nat. Med.* (2020). doi:10.1038/s41591-020-0822-7

433 2. COVID-19 Data Explorer - Our World in Data. Available at:
434 https://ourworldindata.org/explorers/coronavirus-data-
435 explorer?zoomToSelection=true&time=2020-03-
436 01..latest&country=USA~GBR~CAN~DEU~ITA~IND&region=World&pickerMetric=l
437 ocation&pickerSort=asc&Metric=Confirmed+cases&Interval=7-
438 day+rolling+average&Align+outbreaks=false&Relative+to+Population=true.
439 (Accessed: 19th June 2021)

440 3. Different COVID-19 Vaccines | CDC. Available at:
441 https://www.cdc.gov/coronavirus/2019-ncov/vaccines/different-vaccines.html.
442 (Accessed: 19th March 2021)

443 4. Safe COVID-19 vaccines for Europeans | European Commission. Available at:
444 https://ec.europa.eu/info/live-work-travel-eu/coronavirus-response/safe-covid-
445 19-vaccines-europeans_en. (Accessed: 19th March 2021)

446 5. Böttcher, L. & Nagler, J. Decisive Conditions for Strategic Vaccination against
447 SARS-CoV-2. *medRxiv* 2021.03.05.21252962 (2021).
448 doi:10.1101/2021.03.05.21252962

449 6. Walsh, E. E., Shin, J. H. & Falsey, A. R. Clinical impact of human coronaviruses
450 229E and OC43 infection in diverse adult populations. *J. Infect. Dis.* (2013).
451 doi:10.1093/infdis/jit393

452 7. Vaccines – COVID19 Vaccine Tracker. Available at:
453 https://covid19.trackvaccines.org/vaccines/. (Accessed: 19th March 2021)

454 8. Tegally, H. *et al.* Emergence and rapid spread of a new severe acute respiratory
455 syndrome-related coronavirus 2 (SARS-CoV-2) lineage with multiple spike
456 mutations in South Africa. *medRxiv* **10**, 2020.12.21.20248640 (2020).

457 9. Rambaut, A. *et al.* Preliminary genomic characterisation of an emergent SARS-
458 CoV-2 lineage in the UK defined by a novel set of spike mutations - SARS-CoV-2
459 coronavirus / nCoV-2019 Genomic Epidemiology - Virological. (2020). Available at:
460 https://virological.org/t/preliminary-genomic-characterisation-of-an-emergent-
461 sars-cov-2-lineage-in-the-uk-defined-by-a-novel-set-of-spike-mutations/563.
462 (Accessed: 16th April 2021)

463 10. Wang, P. *et al.* Increased Resistance of SARS-CoV-2 Variants B.1.351 and B.1.1.7
464 to Antibody Neutralization. *bioRxiv Prepr. Serv. Biol.* (2021).
465 doi:10.1101/2021.01.25.428137

466 11. Luchsinger, L. L. & Hillyer, C. D. Vaccine efficacy probable against COVID-19
467 variants. *Science (80-.).* **371**, 1116 LP – 1116 (2021).

468 12. Starr, T. N. *et al.* Prospective mapping of viral mutations that escape antibodies
469 used to treat COVID-19. *Science (80-.).* **371**, 850–854 (2021).

470 13. Starr, T. N. *et al.* Deep Mutational Scanning of SARS-CoV-2 Receptor Binding
471 Domain Reveals Constraints on Folding and ACE2 Binding. *Cell* **182**, 1295-
472 1310.e20 (2020).

473 14. Greaney, A. J. *et al.* Complete Mapping of Mutations to the SARS-CoV-2 Spike
474 Receptor-Binding Domain that Escape Antibody Recognition. *Cell Host Microbe*
475 **29**, 44-57.e9 (2021).

476 15. Thompson, R. N., Hill, E. M. & Gog, J. R. SARS-CoV-2 incidence and vaccine escape.
477 *Lancet Infect. Dis.* (2021). doi:10.1016/S1473-3099(21)00202-4

478 16. Gerrish, P. J. *et al.* How unequal vaccine distribution promotes the evolution of
479 vaccine escape. *medRxiv* (2021).

480 17. Cobey, S., Larremore, D. B., Grad, Y. H. & Lipsitch, M. Concerns about SARS-CoV-2
481 evolution should not hold back efforts to expand vaccination. *Nature Reviews*
482 *Immunology* 1–6 (2021). doi:10.1038/s41577-021-00544-9

483 18. Geoffroy, F., Traulsen, A. & Uecker, H. Vaccination strategies when vaccines are
484 scarce: On conflicts between reducing the burden and avoiding the evolution of
485 escape mutants. *medRxiv* 2021.05.04.21256623 (2021).
486 doi:10.1101/2021.05.04.21256623

487 19. Baker, R. E., Yang, W., Vecchi, G. A., Metcalf, C. J. E. & Grenfell, B. T. Assessing the
488 influence of climate on wintertime SARS-CoV-2 outbreaks. *Nat. Commun.* **12**, 1–7
489 (2021).

490 20. Geoghegan, J. L. *et al.* Genomic epidemiology reveals transmission patterns and
491 dynamics of SARS-CoV-2 in Aotearoa New Zealand. *Nat. Commun.* **11**, 1–7 (2020).

492 21. Komissarov, A. B. *et al.* Genomic epidemiology of the early stages of the SARS-
493 CoV-2 outbreak in Russia. *Nat. Commun.* **12**, 1–13 (2021).

494 22. Faria, N. R. *et al.* Genomics and epidemiology of the P.1 SARS-CoV-2 lineage in
495 Manaus, Brazil. *Science (80-.).* eabh2644 (2021). doi:10.1126/science.abh2644

496 23. Lythgoe, K. A. *et al.* SARS-CoV-2 within-host diversity and transmission. *Science*
497 *(80-.).* **372**, eabg0821 (2021).

498 24. Komarova, N. L., Schang, L. M. & Wodarz, D. Patterns of the COVID-19 pandemic
499 spread around the world: Exponential versus power laws: Patterns of the COVID-
500 19 pandemic spread around the world: Exponential versus power laws. *J. R. Soc.*
501 *Interface* **17**, (2020).

502 25. Saad-Roy, C. M. *et al.* Immune life history, vaccination, and the dynamics of SARS-
503 CoV-2 over the next 5 years. *Science (80-.).* **370**, 811–818 (2020).

504 26. BERNOULLI & D. Essai d'une nouvelle analyse de la mortalite causee par la petite
505 verole, et des avantages de l'inoculation pour la prevenir. *Hist. l'Acad., Roy. Sci.*
506 *avec Mem* 1–45 (1760).

507 27. Kermack, W. 0 & Mckendrick, A. G. A contribution to the mathematical theory of
508 epidemics. *Proc. R. Soc. London. Ser. A, Contain. Pap. a Math. Phys. Character*

115, 700–721 (1927).

28. Diekmann, O., Heesterbeek, J. A. P. & Metz, J. A. J. On the definition and the computation of the basic reproduction ratio R0 in models for infectious diseases in heterogeneous populations. *J. Math. Biol.* **28**, 365–382 (1990).

29. Dietz, K. The estimation of the basic reproduction number for infectious diseases. *Stat. Methods Med. Res.* **2**, 23–41 (1993).

30. Nowak, M. A. & May, R. M. Superinfection and the evolution of parasite virulence. *Proc. R. Soc. B Biol. Sci.* **255**, 81–89 (1994).

31. Nowak, M. A. & Bangham, C. R. M. Population dynamics of immune responses to persistent viruses. *Science (80-.).* **272**, 74–79 (1996).

32. Hethcote, H. W. Mathematics of infectious diseases. *SIAM Rev.* **42**, 599–653 (2000).

33. Brauer, F. & Castillo-Chavez, C. *Mathematical Models in Population Biology and Epidemiology*. **40**, (Springer New York, 2012).

34. Hamer, W. The Milroy Lectures ON EPIDEMIC DISEASE IN ENGLAND-THE EVIDENCE OF VARIABILITY AND OF PERSISTENCY OF TYPE. *The Lancet* **167**, 569–574 (1906).

35. Bailey, N. *The Mathematical Theory of Infectious Diseases and its applications*. *Immunology* **34**, (Wiley-Blackwell, 1978).

36. Tillett, H. E. Infectious Diseases of Humans; Dynamics and Control. *Epidemiol. Infect.* **108**, 211 (1992).

37. Nowak, M. & May, R. M. Virus Dynamics: Mathematical Principles of Immunology And Virology. Available at: https://www.researchgate.net/publication/48378467_Virus_Dynamics_Mathematical_Principles_of_Immunology_And_Virology. (Accessed: 30th March 2021)

534 38. Diekmann, O. & Heesterbeek, J. A. P. Mathematical Epidemiology of Infectious
535 Diseases: Model Building, Analysis and Interpretation. Available at:
536 https://www.researchgate.net/publication/48376881_Mathematical_Epidemiolo
537 gy_of_Infectious_Diseases_Model_Building_Analysis_and_Interpretation.
538 (Accessed: 30th March 2021)

539 39. Ragonnet-Cronin, M. *et al.* Genetic evidence for the association between COVID-
540 19 epidemic severity and timing of non-pharmaceutical interventions. *Nat.*
541 *Commun.* **12**, 2188 (2021).

542 40. Rossman, H. *et al.* Hospital load and increased COVID-19 related mortality in
543 Israel. *Nat. Commun.* **12**, 1904 (2021).

544 41. Saad-Roy, C. M. *et al.* Epidemiological and evolutionary considerations of SARS-
545 CoV-2 vaccine dosing regimes. *Science (80-.).* eabg8663 (2021).
546 doi:10.1126/science.abg8663

547 42. Saad-Roy, C. M. *et al.* Immune life history, vaccination, and the dynamics of SARS-
548 CoV-2 over the next 5 years. *Science (80-.).* **370**, 811–818 (2020).

549 43. Ashcroft, P., Lehtinen, S., Angst, D. C., Low, N. & Bonhoeffer, S. Quantifying the
550 impact of quarantine duration on covid-19 transmission. *Elife* **10**, 1–33 (2021).

551 44. Komarova, N. L., Azizi, A. & Wodarz, D. Network models and the interpretation of
552 prolonged infection plateaus in the COVID19 pandemic. *Epidemics* 100463 (2021).
553 doi:10.1016/j.epidem.2021.100463

554 45. Castro, M., Ares, S., Cuesta, J. A. & Manrubia, S. The turning point and end of an
555 expanding epidemic cannot be precisely forecast. *Proc. Natl. Acad. Sci.* **117**,
556 26190–26196 (2020).

557 46. Stich, M., Manrubia, S. C. & Lázaro, E. Variable mutation rates as an adaptive
558 strategy in replicator populations. *PLoS One* (2010).
559 doi:10.1371/journal.pone.0011186

47. Yagan, O. *et al.* Modeling and Analysis of the Spread of COVID-19 Under a Multiple-Strain Model with Mutations. *Harvard Data Sci. Rev.* (2021). doi:10.1162/99608f92.a11bf693

48. Lehtinen, S., Ashcroft, P. & Bonhoeffer, S. On the relationship between serial interval, infectiousness profile and generation time. *J. R. Soc. Interface* (2021). doi:10.1098/rsif.2020.0756

49. Hethcote, H. W. Three Basic Epidemiological Models. in (1989). doi:10.1007/978-3-642-61317-3_5

50. Gillespie, D. T. A general method for numerically simulating the stochastic time evolution of coupled chemical reactions. *J. Comput. Phys.* **22**, 403–434 (1976).

51. Gillespie, D. T. Exact stochastic simulation of coupled chemical reactions. in *Journal of Physical Chemistry* **81**, 2340–2361 (American Chemical Society, 1977).

52. Cota, W. & Ferreira, S. C. Optimized Gillespie algorithms for the simulation of Markovian epidemic processes on large and heterogeneous networks. *Comput. Phys. Commun.* **219**, 303–312 (2017).

53. Mukhamadiarov, R. I. *et al.* Social distancing and epidemic resurgence in agent-based susceptible-infectious-recovered models. *Sci. Rep.* **11**, 130 (2021).

METHODS

Derivation of mathematical results

1. No Vaccination

First we consider the case without vaccination. We denote by x the number of susceptible individuals; by y the number of individuals infected with wildtype (WT); by z the number of individuals recovered from WT. The infection rate is β; the recovery rate a ; the mutation rate μ; the population size N. The social activity parameter $s(t)$ captures the

extent of imposed lockdown that varies over time. For simplicity, we neglect the number of individuals who die, hence the population size N is assumed to be constant.

Deterministic WT infection dynamics are given by the system of differential equations:

$$\begin{aligned} \dot{x} &= -\beta s x y \\ \dot{y} &= \beta s x y - a y \\ \dot{z} &= a y \end{aligned} \tag{7}$$

Initially, all of the population is susceptible to the WT strain, and no individuals are infected with or recovered from the WT strain. Therefore, we have: $x(0) = N$, $y(0) = 0$ and $z(0) = 0$. Social activity, $s(t)$, is adjusted such that $y(t) = L/a$ is constant (see **Figure S2C**). L is the number of new infections per day.

Without lockdown, $s = 1$, the basic reproductive ratio of the WT is given by $R_0 = \beta N/a$. If $R_0 > 1$, the number of infected individuals grows initially. With lockdown, $s < 1$, the reproductive ratio is $R_{WT} = \beta N s/a$. Since the social distancing measures maintain $y(t) = L/a$ at a constant value, we have $R_{WT} = 1$ and $\beta s(t) x(t) = a$ (see **Figure S2**). The parameter s can vary between 0 and 1.

Each day, L individuals become infected and L individuals recover. Therefore, we have:

$$\begin{aligned} \dot{x} &= -L \\ \dot{y} &= 0 \\ \dot{z} &= L \end{aligned} \tag{8}$$

The solution to this system of differential equations is

$$\begin{aligned} x(t) &= N - Lt \\ z(t) &= Lt \end{aligned} \tag{9}$$

Hence, the number of susceptible individuals decreases linearly with slope L while the number of recovered individuals increases linearly with slope L. (See **Figure S2** for agreement with the stochastic simulation).

When $x(t)$ has declined such that $R_{WT} < 1$ and $s = 1$, there are not enough susceptible individuals to sustain the infection. This herd immunity is achieved when $x(t) < a/\beta$. Thus, the time T_H until herd immunity is given by $\beta(N - Lt) = a$. We obtain:

$$T_H = \frac{N}{L}\left(1 - \frac{1}{R_0}\right) \tag{10}$$

1.1 Rate of generating mutants

Each day, L new individuals become infected. Each of these infections has probability μ to be a vaccine-resistant MT. Hence, the rate of producing a mutant is $L\mu$ per day. Let $P(t)$ denote the probability that no mutant has been produced until time t. We have $\dot{P(t)} = -L\mu P(t)$, which leads to $P(t) = e^{-L\mu t}$.

The MT strain can be generated only during infection. Hence, if the MT strain has not been generated until the time when there are no more WT infections – that is, approximately when herd immunity is reached – it will never be generated. We neglect here the time of exponential decrease in the number of WT infections between time T_H (when herd immunity is reached) and the time when the number of WT infections has reached zero. The probability that no mutant will appear before time T_H is $P(T_H) = e^{-L\mu T_H}$. Inserting from eq (4) we obtain

$$P(T_H) = \exp(-N\mu(1 - 1/R_0) \tag{11}$$

1.1 Rate of generating surviving mutants

In order to calculate the probability that the MT strain will be generated and survive, we need to multiply the rate of generation of the MT strain with the probability that it will not become extinct by random drift. If $\rho(t)$ is the survival probability of the MT, then the rate of producing a surviving mutant is $L\mu\rho(t)$ per day. We approximate $\rho(t) = 1 - 1/R_{MT}(t)$, where $R_{MT}(t)$ is the reproductive ratio of the mutant at time T.

We have

$$R_{MT}(t) = \beta s(t)N/a \tag{12}$$

Since $s(t) = a/\beta x(t)$ and using Eq. (9) we obtain

$$R_{MT}(t) = \frac{N}{N - Lt} \tag{13}$$

And therefore we have $\rho(t) = Lt/N$.

Let $P(t)$ denote the probability that not surviving mutant has been produced until time t. We have $\dot{P(t)} = -L\mu\rho(t)P(t) = -L^2\mu t P(t)/N$. We can solve this differential equation to obtain $P(t) = \exp(-\mu L^2 t^2/2N)$. The probability that no surviving mutant has been produced until herd immunity, which is reached at time T_H, is given by

$$P(T_H) = \exp(-\frac{\mu N}{2}\left(1 - \frac{1}{R_0}\right)^2) \tag{14}$$

2. With Vaccination

Let us now add vaccination. Denote by w the number of vaccinated people. If both recovered and susceptible individuals are vaccinated at a total rate of c per day then deterministic infection and vaccination dynamics are given by

$$\begin{aligned} \dot{x} &= -\beta sxy - \frac{cx}{x+z} \\ \dot{y} &= \beta sxy - ay \\ \dot{z} &= ay - \frac{cz}{x+z} \\ \dot{w} &= c \end{aligned} \tag{15}$$

The initial condition is $x(0) = N$, $y(0) = 0$, $z(0) = 0$, $w(0) = 0$, $s(0) = 1$ and $R_0 = \beta N/a$. As before, we adjust $s(t)$ such that $y(t) = L/a$ is constant (see **Figure 3**).

Each day, L susceptible individuals become infected and $cx(x+z)$ susceptible individuals become vaccinated. Also, L infected individuals recover, and $cx(x+z)$ of recovered individuals become vaccinated. We have:

$$\dot{x} = -L - \frac{cx}{x+z}$$

$$\dot{y} = 0$$

$$\dot{z} = L - \frac{cz}{x+z} \tag{16}$$

$$\dot{w} = c$$

For simplicity let us assume that we only vaccinate susceptible people. This assumption is a reasonable approximation if $c \gg L$. In this case, we can write

$$\dot{x} = -L - c$$

$$\dot{y} = 0$$

$$\dot{z} = L \tag{17}$$

$$\dot{w} = c$$

The solution to this system of differential equations is

$$x(t) = N - Lt - ct$$

$$z(t) = Lt \tag{18}$$

$$w(t) = ct$$

Hence, the number of susceptible individuals decreases linearly with slope $L + c$, while the number of recovered individuals increases linearly with slope L, and the number of vaccinated individuals increases linearly with slope c.

The time T_H until herd immunity is given by

$$T_H = \frac{N}{c+L}(1 - 1/R_0) \tag{19}$$

2.1 Rate of generating mutants

The rate of producing a mutant is $L\mu$ per day. Let $P(t)$ denote the probability that no mutant has been produced until time t. We have $\dot{P(t)} = -L\mu P(t)$, which gives $P(t) = \exp(-L\mu t)$.

The MT strain can be generated only during infection. Hence, if the MT strain has not been generated until the time when there are no more WT infections – that is, when herd immunity is reached – it will never be generated. Again we neglect here the time of exponential decrease in the number of WT infections between the time T_H when herd immunity is reached and the time where the number of WT infections reaches 0. Hence, the probability that no mutant will appear is $P(T_H) = \exp(-L\mu T_H)$. Using Eq. (19), the probability that no mutant has appeared until herd immunity is:

$$P(T_H) = \exp(-N\mu\left(\frac{L}{c+L}\right)\left(1-\frac{1}{R_0}\right)) \tag{20}$$

2.2 Rate of generating surviving mutants

In order to calculate the probability that surviving mutants are generated, we again consider the survival probability $\rho(t) = 1 - 1/R_{MT}(t)$, where $R_{MT}(t)$ is the reproductive ratio of the mutant at time t. The rate of producing a surviving mutant is then $L\mu\rho(t)$ per day. We have:

$$R_{MT}(t) = \frac{\beta s(t)N}{a} \tag{21}$$

As explained above, $s(t) = a/\beta x(t)$. Using Eq. (18) we obtain

$$R_{MT}(t) = \frac{N}{N-(L+c)t} \tag{22}$$

And therefore $\rho(t) = (L+c)t/N$.

Let $P(t)$ denote the probability that not surviving mutant has been produced until time t. We have $\dot{P(t)} = -L\mu\rho(t)P(t) = -L\mu(c+L)tP(t)/N$. Let $v = c/N$ and $l = L/N$. We can solve this differential equation to obtain:

$$P(t) = \exp(-\frac{\mu N}{2} l(v+l)t^2) \tag{23}$$

The probability that no surviving mutant has been produced until herd immunity, which is reached at time T_H, is:

$$P(T_H) = \exp(-\frac{\mu N}{2}(\frac{l}{v+l})\left(1-\frac{1}{R_0}\right)^2) \tag{24}$$

2.3 Rate of generating surviving mutants with partial immune escape

We can also study the case where the infectivity of the mutants is reduced by a factor $q \epsilon [0,1]$ when infecting recovered or vaccinated people. For $q = 1$ we obtain full escape, while $q = 0$ means that the mutant does not escape at all.

A similar derivation to the one above leads to the following result. The probability that no surviving mutant with partial escape q has appeared until herd immunity is given by:

$$P(T_H) = \exp(-\frac{\mu N}{2}(\frac{l}{v+l})A)$$

$$\text{with} \qquad A = \frac{2q}{1-q}(-\frac{R_0-1}{R_0} + \frac{1}{1-q}\log\frac{R_0}{1+q(R_0-1)}) \tag{25}$$

For $q = 1$ we obtain $A = (1-(1/R_0))^2$ leading to Eq. (23) above.

Relationship between the product formula and the exponential formula

Each day, L new WT infections occur. Each new infection has a probability of μ to be the MT strain. The survival probability of the mutant is approximately $1 - 1/R_m(t)$ where $R_m(t)$ is the basic reproductive ratio of the MT appearing at time t.

Hence, the probability that none of the L new WT infections in a day will generate a surviving mutant is $(1 - \mu(1 - 1/R_m(t)))^L$. Then, we can write the probability P that no surviving mutant will be produced between time $t = 0$ and the time T_H when herd immunity is reached as the product

$$P = \prod_{\tau=0}^{T_H} [1 - \mu\left(1 - \frac{1}{R_{MT}(\tau)}\right)]^L \tag{26}$$

We have $T_H = [N/(c + L)](1 - 1/R_0)$ and $R_{MT}(t) = N/[N - (c + L)t]$.

Since $\rho(t) = 1 - 1/R_m(t) = (c + L)t/N$ we can write:

$$P = \prod_{\tau=0}^{T_H} (1 - \frac{\mu(c + L)\tau}{N})^L$$

Let us use the abbreviation $u = \mu(c + L)/N$. Then

$$P = \prod_{\tau=0}^{T_H} (1 - u\tau)^L$$

$$= \exp[log \prod_{\tau=0}^{T_H} (1 - u\tau)^L]$$

$$= \exp[L\ log \prod_{\tau=0}^{T_H} (1 - u\tau)]$$

$$= \exp[L \sum_{\tau=0}^{T_H} \log(1 - u\tau)] \tag{27}$$

Note that Eq. (26) is exactly equivalent to Eq. (23). Assuming $uT_H \ll 1$ which is the same as $\mu(1 - (1/R_0)) \ll 1$ we obtain

$$P = \exp[-uL\sum_{\tau=0}^{T_H}\tau]$$

$$= \exp\left[-\frac{uLT_H(T_H+1)}{2}\right]$$

Assuming $T_H \gg 1$ which is $N\left(1-\frac{1}{R_0}\right) \gg c+L$, we obtain

$$P = \exp\left[-\frac{uL{T_H}^2}{2}\right]$$

$$= \exp\left[-\frac{(\mu(c+L)/N)L{T_H}^2}{2}\right]$$

Finally, inserting $T_H = (N/(c+L))(1-1/R_0)$ we get:

$$P(T_H) = \exp(-\frac{\mu N}{2}(\frac{l}{v+l})\left(1-\frac{1}{R_0}\right)^2) \tag{28}$$

Which is equivalent to Eq.(24) (see above).

Dynamics after appearance of the MT strain

1. No Vaccination

After the MT strain has taken over, social distancing measures will continue maintaining the number of daily infections at L, which implies that $(y_1+y_2) = L/a$ (see **Figure S2**). In practice, the WT strain rapidly goes extinct upon emergence of the MT strain; so we can consider $y_2 = L/a$ .The mutant strain can infect susceptible individuals x, and recovered individuals, z_1. The mutant strain infects those individuals with probabilities proportional to their frequencies at the time $t^*$of mutant takeover. Hence, for times $t > t^*$ we have:

$$x(t) = x(t^*) - \frac{x(t^*)}{z_1(t^*)+x(t^*)}L(t^*-t)$$

$$z_1(t) = z_1(t^*) - \frac{z_1(t^*)}{z_1(t^*)+x(t^*)}L(t^*-t) \tag{29}$$

After mutant takeover, the social distancing measures need to be readjusted to the mutant strain. Since more individuals are susceptible to it, $s(t)$ has to decrease (see **Figure S2F**):

$$s(t) = \frac{aN}{\beta(x(t) + qz_1(t))} \tag{30}$$

Which implies that $R_{MT} = 1$.

2. With vaccination

As for the case without vaccination, if the mutant strain survives, it will quickly replace the wild-type strain such that $y_2 = L/a$ (see **Figure 3C**). The number of susceptible individuals $x(t^*)$ at time of mutant takeover can be neglected for large enough vaccination rates. The number of vaccinated individuals, susceptible to the mutant strain w_1 will hence decrease linearly with the number of tolerated cases per day L, and the number of vaccinated individuals, recovered from the mutant strain w_2 will increase complementarily linearly with L. If the mutant takes over at time t^*, we have for all times $t > t^*$:

$$\begin{aligned} w_1(t) &= w_1(t^*) - L(t^* - t) \\ w_2(t) &= L(t^* - t) \end{aligned} \tag{31}$$

The social activity parameter s needs readjustment to consider the additional groups of individuals that are now susceptible to the infecting strain. We have:

$$s(t) = \frac{a}{\beta} \frac{x(t) + q(z_1(t) + w_1(t)}{x(t) + q(z_1(t) + w_1(t)) - w_2(t)} \tag{32}$$

Which ensures that $R_{MT} = 1$. Here the parameter q in $[0,1]$ denotes the extent of escape.

Estimating the evolutionary potential of the virus

If μ is the mutation rate as described above and $L(t)$ is the time series giving the number of new infections on day t, then the probability that no mutant has been produced between time 0 and time T_H is given by:

$$P(T_H) = \prod_{\tau=0}^{T_H} [1-\mu]^{L(\tau)} \tag{33}$$

This probability will overestimate the evolutionary potential of the virus to escape from vaccination because many mutants do not survive the initial random drift. The probability that no surviving mutant has been produced between time 0 and time T_H can be written as:

$$P(T_H) = \prod_{\tau=0}^{T_H} [1-\mu\rho(\tau)]^{L(\tau)} \tag{34}$$

Here $\rho(t)$ is the survival probability of an escape mutant produced at time t. This probability depends on the basic reproductive ratio of the mutant on the day it is being produced (and the next few days until random drift is negligible). Approximately we can write:

$$\rho(t) = \min\{0,1-\frac{1}{R_M(t)}\} \tag{35}$$

For the potential of the virus to generate mutants (irrespective of whether they survive) what matters most is the total number of infections, $\sum_\tau L(\tau)$. But for the potential of the virus to generate surviving mutants one must also consider the time periods when lockdown is relaxed such that R_{MT} is above 1.

GILLESPIE PSEUDOCODE

```
Time = 0
```

```
Day = 0
Initialize population
Initialize reaction rates
while (y_1 + y_2A + y_2B > 0):
    if day passed:
        day = day + 1
        if number infections in previous day > L:
            s = s - random number, uniform distribution [0, 0.1]
        if number infections in previous day < L:
            s = s + random number, uniform distribution [0, 0.1]
    r1 = random number from uniform distribution between 0 and 1
    r2 = random number from uniform distribution between 0 and 1
    alpha = sum(reaction_rates)
    tau = 1/alpha ln(1/r1)
    time = time + tau
    choose reaction, probability proportional to their rates and r2*alpha
    update population according to chosen reaction
    update reaction rates
    record population
```

TABLE OF REACTIONS AND THEIR RATES

Infection		
WT Infected Infects Susceptible	$y_1 + 1; x - 1$	$\beta_1 s x y_1$
VR (unvaccinated) Infects Susceptible	$y_{2A} + 1; x - 1$	$\beta_2 s x y_{2A}$
VR (unvaccinated) Infects Recovered from WT	$y_{2A} + 1; z_1 - 1$	$q\beta_2 s z_1 y_{2A}$
VR (unvaccinated) Infects Vaccinated	$y_{2B} + 1; w_1 - 1$	$q\beta_2 s w_1 y_{2A}$
VR (vaccinated) Infects Susceptible	$y_{2A} + 1; x - 1$	$\beta_2 s x y_{2B}$
VR (vaccinated) Infects Recovered from WT	$y_{2A} + 1; z_1 - 1$	$q\beta_2 z_1 s y_{2B}$
VR (vaccinated) Infects Vaccinated	$y_{2B} + 1; w_1 - 1$	$q\beta_2 w_1 s y_{2B}$
Mutation		

WT Mutates into VR	$x-1; y_{2A}+1$	$\beta_1 s x y_1 \mu$
Recovery		
WT Infected Recovers	$y_1-1; z_1+1$	$a y_1$
VR unvaccinated Recovers	$y_{2A}-1; z_2+1$	$a y_{2A}$
VR vaccinated Recovers	$y_{2B}-1; w_2+1$	$a y_{2B}$
Death		
WT Infected Dies	y_1-1	$d y_1$
VR unvaccinated Dies	$y_{2A}-1$	$d y_{2A}$
VR vaccinated Dies	$y_{2B}-1$	$d y_{2B}$
Vaccination		
Susceptible Gets Vaccinated	$x-1; w_1+1$	$\frac{cx}{(x+z_1+z_2)}$
WT Recovered Gets Vaccinated	$z_1-1; w_1+1$	$\frac{cz_1}{(x+z_1+z_2)}$
WT and VR Recovered Gets Vaccinated	$z_2-1; w_2+1$	$\frac{cz_2}{(x+z_1+z_2)}$

SUPPLEMENTARY FIGURES

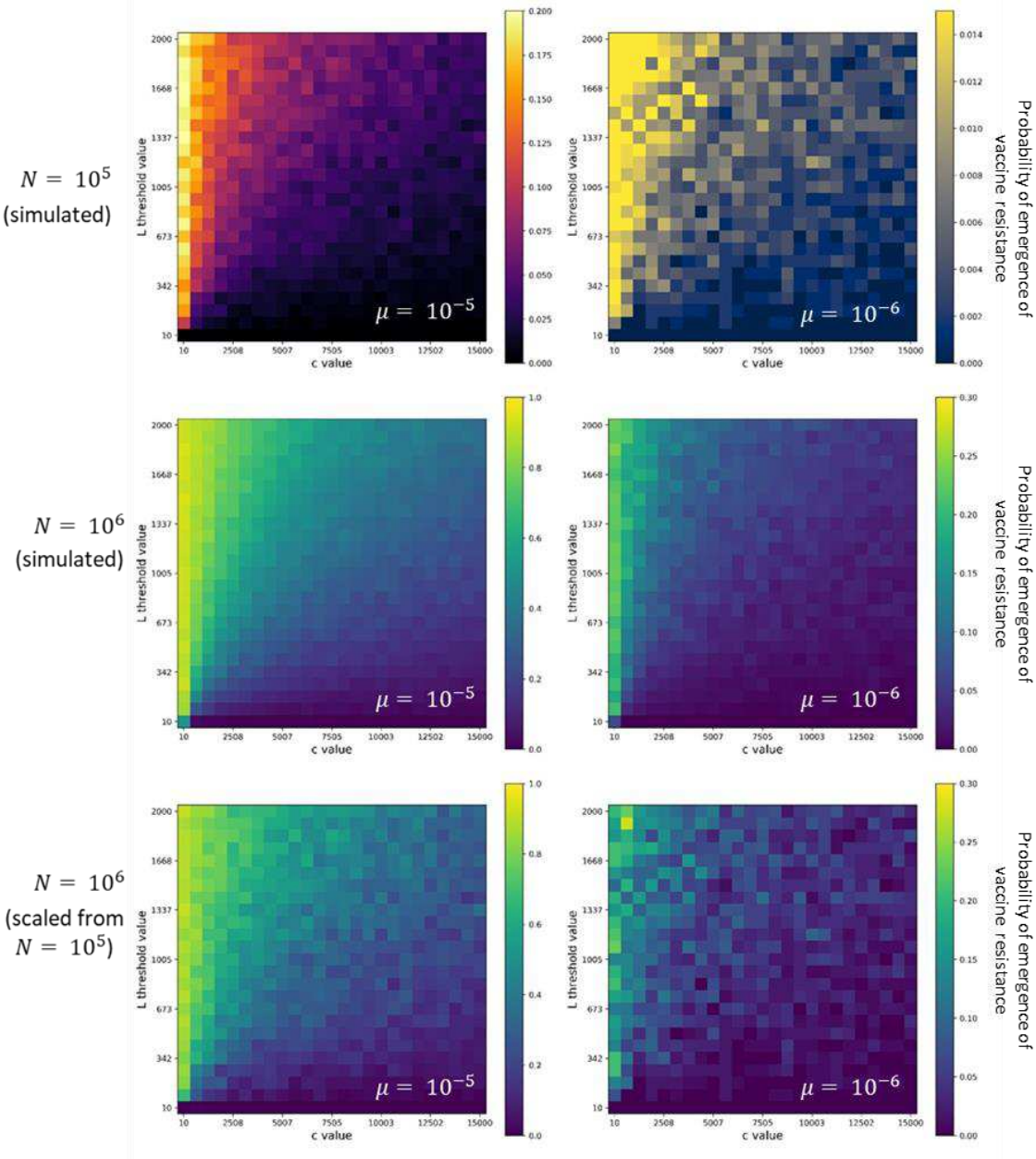

Figure S1: Scaling simulation results to larger population sizes. Results of simulations for a given population size can be scaled to larger population size according to $1 - (1 - p)^m$, where p is the proportion of runs where the MT strain took over and m the ratio of the scaled population size to the simulated population size. (A) (B) Each square of the color map is colored according to the proportion of runs (out of 100) where the MT strain took over for $N = 10^5$. (C) (D) Each square of the color map is colored according to

$1-(1-p)^{10}$, where p is the proportion of runs where the MT strain took over in simulations presented in (A) and (B). (E) (F) Each square of the color map is colored according to the proportion of runs (out of 100) where the MT strain took over for $N = 10^6$. We observe a good agreement between the scaled results and the simulated results.

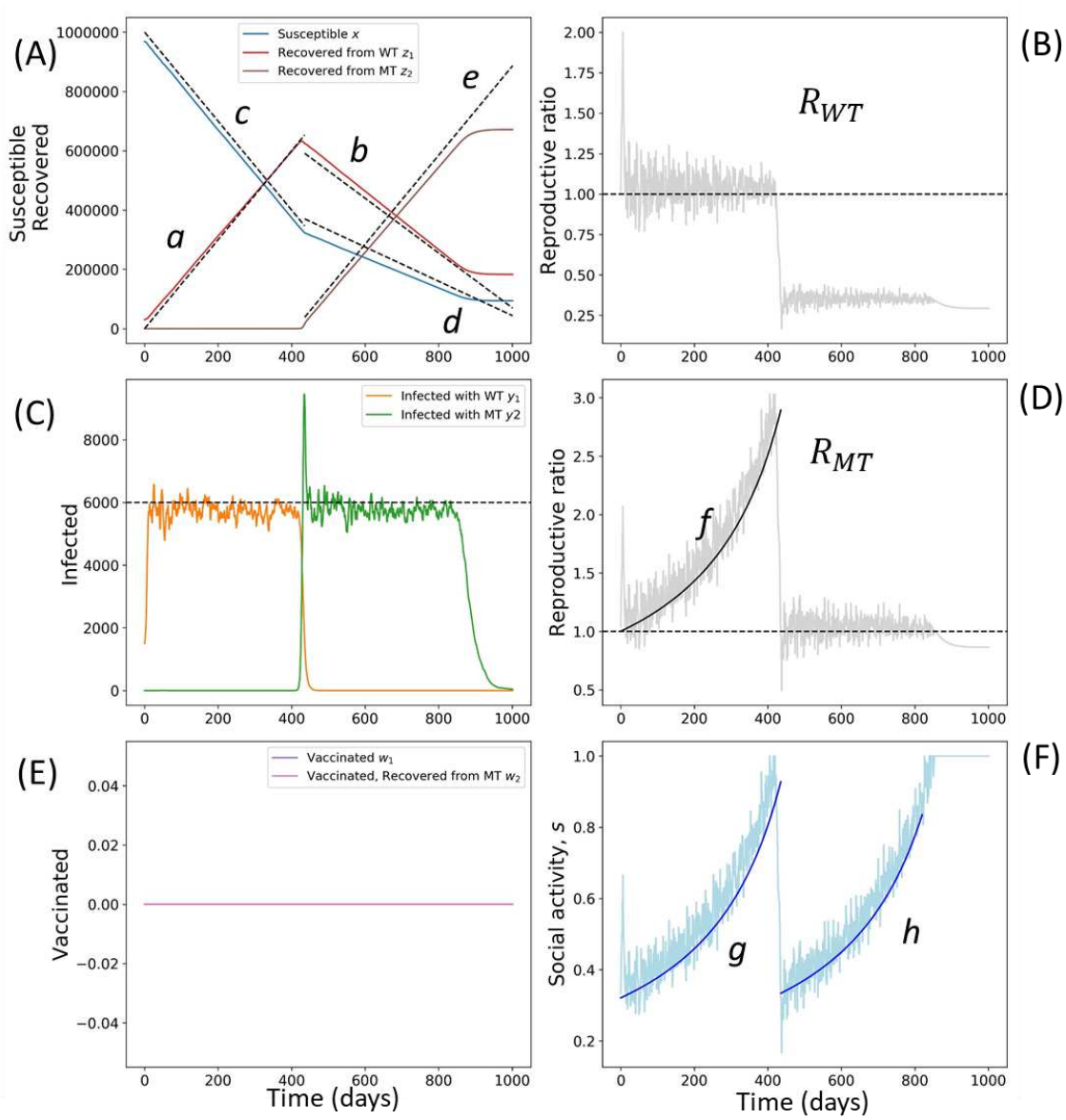

Figure S2: Evolution of resistance in absence of vaccination. (A) Before MT takeover, the decline in susceptible individuals (x) along time can be approximated by a linear function with slope equal to L. Since we assume no vaccination, the number of individuals recovered from WT grows linearly with slope equal to L. After MT takeover, the number of individuals recovered from MT grows linearly slope equal to L, while the number of susceptible individuals (x) and individuals recovered from WT (z_1) declines linearly with a slope proportional to their frequencies at the moment of MT takeover. The equations of the lines (a), (b),

(c), (d) and (e) are given by, with t^* the time of takeover by the mutant strain: (a) $z_1(t) = z_1(0) + Lt,\ t < t^*$ (b) $z_1(t) = (z_1(t^*) - z_1(t^*)/(z_1(t^*) + x(t^*)))L(t^* - t), t > t^*$ (c) $x(t) = x(0) - Lt, t < t^*$ (d) $x(t) = x(t^*) - (x(t^*)/(z_1(t^*) + x(t^*)))L(t^* - t), t > t^*$ (e) $z_2(t) = L(t^* - t),\ \ t > t^*$. (B) The reproduction coefficient of the wild-type R_{WT} is maintained at 1 by the dynamic lockdown. After mutant takeover, R_{WT} is less than 1, since the lockdown is now adjusted to the population susceptible to the MT strain. (C) The number of active cases of WT (y_1) and after mutant takeover, MT (y_1) is constant at L/a until herd immunity to the MT strain is reached. (D) Before MT takeover, the reproductive rate of the MT grows as (b) $R_{MT} = \beta_2(x(t) + z_1(t))/a$. After takeover, R_{MT} is maintained around 1. (E) In this run, there was no vaccination ($c = 0$), hence $w_1 = w_2 = 0$ for each time t. (F) Before MT takeover, the dynamic lockdown is adjusted to the WT. As the number of individuals immune to WT grows, social activity increases. When the MT emerges, lockdown measures are reinstated. Subsequently, social activity increases as the population immune to the MT grows. The equations of the lines are given by (g) $s(t) = a/(\beta_1 x(t)),\ t < t^*$ (h) $s(t) = a/(\beta_2(x(t) + qz_1(t))),\ t > t^*$.

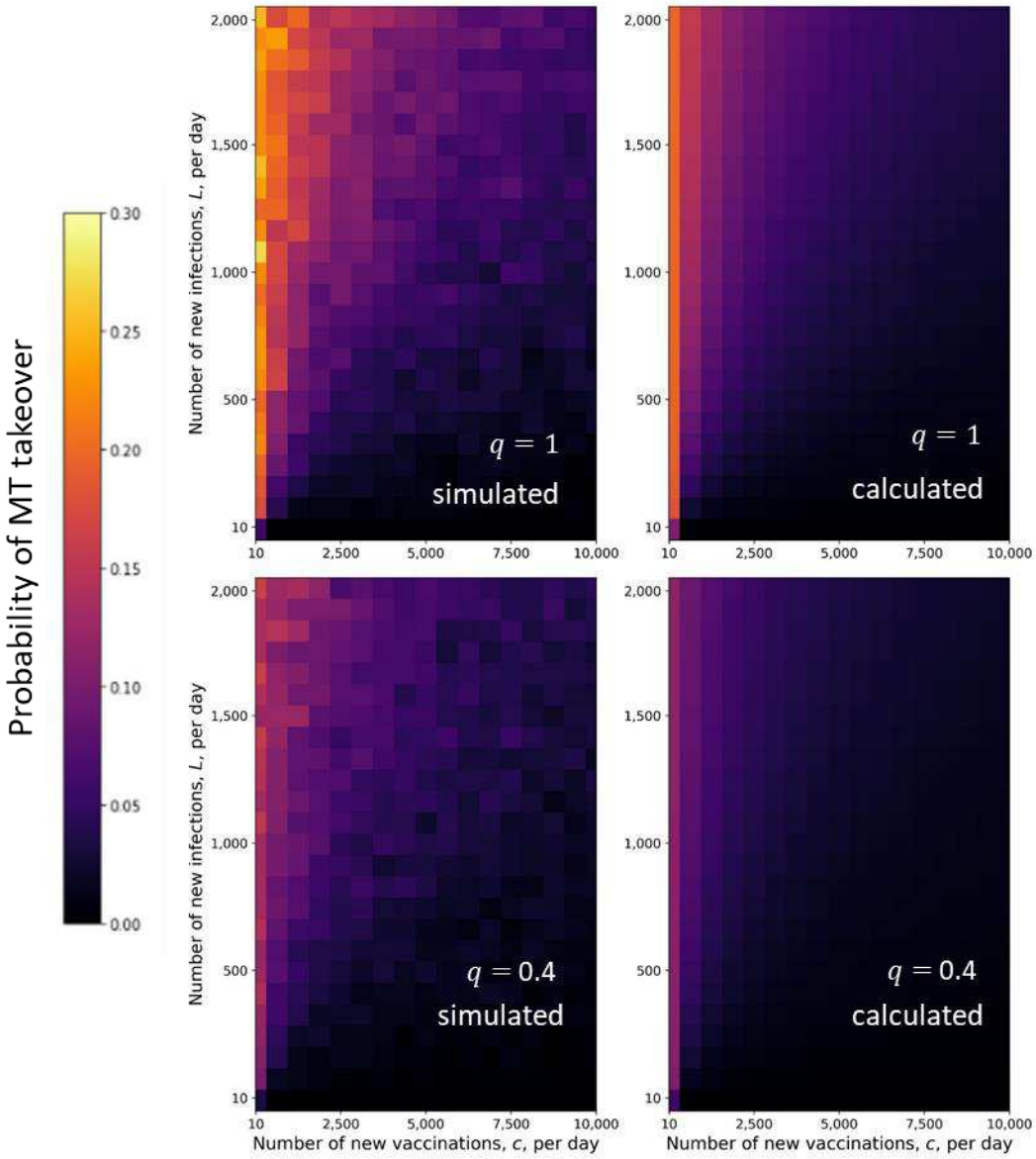

Figure S3: Analytical approximation of the simulation results. The probability of MT takeover before herd immunity is reached can be calculated according to Eq. 5. We observe a good agreement between our calculations and the results of the stochastic simulations. (A) (C) Each square of the color map is colored according to the probability of take over calculated with Eq. (5). (B) (D) Each square of the color map is colored according to the proportion of runs (out of 1000) where the MT strain took over. The population size was $N = 10^6$.

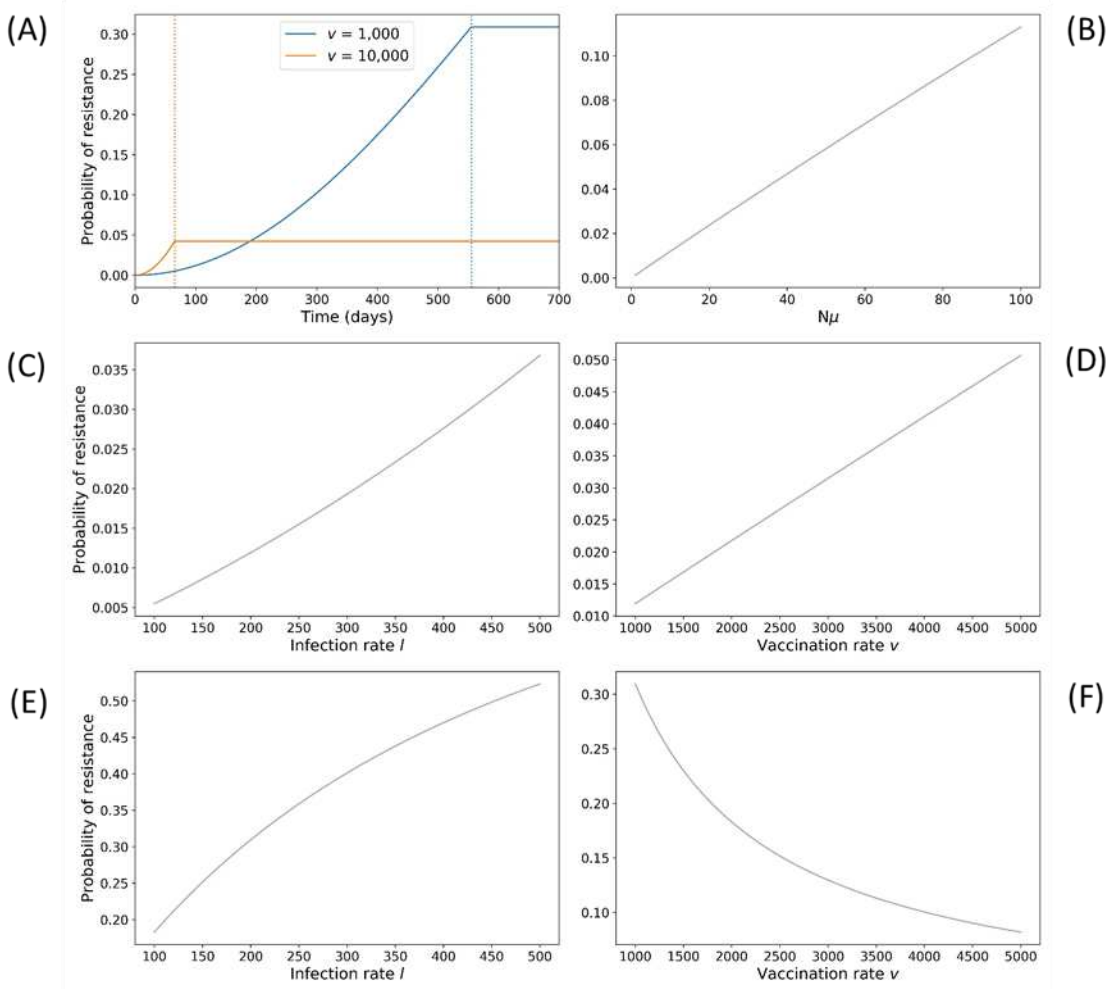

Figure S4: Counterintuitive effect of the vaccination rate on the probability of resistance. Increasing the population size N, the mutation rate μ and the infection rate l all increase the probability of generating a mutant before herd immunity is reached (**B** and **C**). We define $v = c/N$ and $l = L/N$. Increasing the vaccination rate v leads to a counterintuitive effect: the probability for a fixed time increases with v since it leads to faster relaxation of social distancing measures, but it also leads to faster achievement of herd immunity (**A**). Hence the probability of resistance until herd immunity decreases with v (**F**). Parameter values: $\mu = 10^{-7}$ (A): $N = 10^8$, $l = 200 \cdot 10^{-6}$; (B): $l = 200 \cdot 10^{-6}$, $v = 1000 \cdot 10^{-6}$, (C)(E): $N = 10^8$, $v = 1000 \cdot 10^{-6}$; (D)(F): $N = 10^8$, $l = 200 \cdot 10^{-6}$.